Printed in U.S.A.

Paper No.
74-WA/DE-8

an ASME publication

$3.00 PER COPY $1.00 TO ASME MEMBERS

Krishna P. Singh
President and CEO
Holtec International

Burton Paul
Consultant

Stress Concentration in Crowned Rollers

The edges of rollers in needle and roller bearings are crowned (i.e., rounded) in order to prevent large stress concentrations. At present, the crowning radius is determined empirically. In this paper, a numerical solution for the stress concentration in crowned elastic rollers is found. Using this method the true contact region, the load-vs.-compliance relationship, and the peak normal pressure can be determined for any roller geometry. The influence of crown radius on stress concentration is illustrated through numerical examples. This method may profitably be used in the stress analysis and design of a variety of machine elements such as gears, cams, and toothed couplings.

Introduction

If the rolling elements of a roller (or needle) bearing were perfect right cylinders they would make contact along their entire lengths with the outer raceway and the inner raceway (or shaft for some needle bearings). It is apparent that the sharp edges at the ends of such rollers would produce intense stress concentrations beyond the elastic limit. To alleviate this problem the ends of the rollers are rounded, or crowned (see, e.g., [1, 2][1]), as shown in Fig. 1. The precise influence of crowning on the stress distribution and compliance has not yet been mathematically determined.

According to a recent survey of outstanding unsolved research problems in the field of tribology [3], the stress distribution due to crowned rollers is "an extremely important problem, . . . which is highly relevant to the most needed advances in the art of lubrication." In the absence of guidance on this problem from the theory of elasticity, a number of approximate and empirical approaches have been attempted in the past.

Palmgren [4] gave an empirical formula for the diametrical compression of a finite elastic roller of length l (in.), compressed between two elastic half spaces by a force F (1b), where all three bodies are made of identical material. According to Palmgren,

$$\delta_p = A\frac{F^{0.9}}{l^{0.8}} \tag{1}$$

where A depends on elastic properties of the roller (for steel $A = 4.36 \times 10^{-7}$) and δ_p is the diametral contraction of the roller in inches.

Moyar and Morrow [5] state that the lack of an elastic solution of this problem is a major impediment in analyzing the vast wealth of experimental data available on surface failure modes of the bearings. Very recently, engineers at Rollway Bearing Co. are reported to have developed an experimental method of accurately recording the shape of the contact region (see *Machine Design*, April 1972), but no indication is given on how to calculate the associated stresses.

We will show that the three-dimensional problem of the crowned roller can be solved using the formulation described in Singh and Paul [6] or Singh [7]. The method of solution used enables us to explore the following aspects of the problem that have not heretofore been successfully dealt with in the literature: (1) The effect of crowning on the pressure distribution for a given load can be studied, and the best crowning method can be determined for any particular application. (2) The load–deflection relationship of the rollers can be accurately predicted. (3) The stress concentration for any given roller geometry, in general, depends on the load. Since a number of rollers are simultaneously in contact with the raceway at different angular orientations, their radial loads are different. Thus an accurate evaluation of cycling at nonuniform stress levels can be made for use in a theory of cumulative fatigue damage. Without such information the life of the bearing cannot be estimated with sufficient accuracy. (4) Accurate prediction of contact region. This is essential for studies of friction and wear. (5) The elastic properties of both bodies can be arbitrary. The effect of elastic constants on the pressure field can thus be studied using this method.

It is perhaps worthwhile mentioning several aspects of the general problem that are not covered in this paper. For example, we do not pretend that a circular arc gives the "optimum" crown profile, although it should be an excellent approximation to any other smoothly blended profile; the method presented is applicable to any profile. Second, we have not made a detailed numerical study of the many parameter variations that would be necessary to produce detailed design charts, nor do we expect that a reader will be able to make such charts exclusively on the basis of this paper. Such charts can be constructed with the aid of detailed analyses and computer programs, which are fully described in Singh [7]. Similarly, questions of convergence of the numerical method used here may be found in Singh [7], and a proof of uniqueness for the class of problem under discussion has been reported by Kalker [8]. Finally, we note that although we have presented results on surface contact pressures only, it is possible to find subsurface shear

[1] Numbers in brackets designate References at end of paper.

Contributed by the Design Engineering Division for presentation at the Winter Annual Meeting, New York, November 17–22, 1974, of THE AMERICAN SOCIETY OF MECHANICAL ENGINEERS. Manuscript received at ASME Headquarters April 24, 1974. Paper No. 74-WA/DE-8.

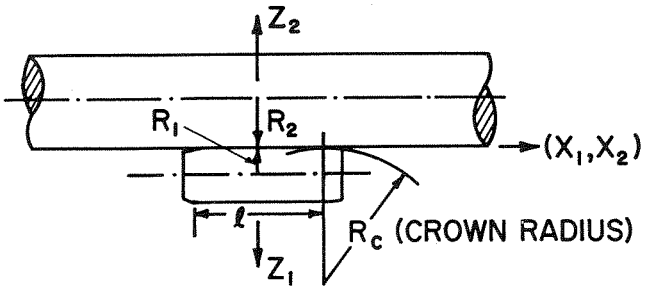

Fig. 1 Crowned roller in contact with a long shaft

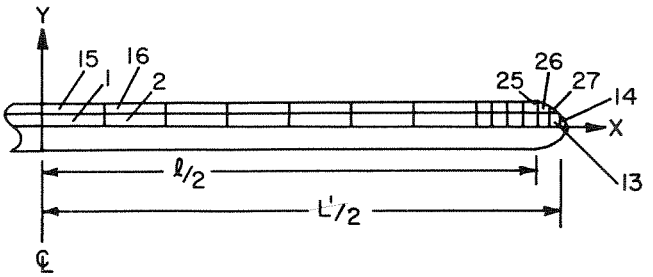

Fig. 2 Contact region, narrow rounded rectangle

or normal stresses (if desired) from a knowledge of the surface loading by utilizing Boussinesq's stress formulae (see [9], p. 364).

Method of Solution

Consider a roller of length l and radius R_1 pressed against a long cylinder of radius R_2, as illustrated in Fig. 1. The ends of the roller are smoothly crowned with a blending radius R_c, henceforth referred to as the crown radius. The crowning arc is tangent to the straight generatrix of the roller. The problem described above is construed to be a typical example. Other crowning contours can also be treated with equal ease by the present method. The contact between the roller and the shaft is initially along a straight line. Upon application of a normal thrust, this line of contact dilates into a narrow rectangle with rounded ends as shown in Fig. 2.

Cartesian coordinate axes (x_1,y_1,z_1) and (x_2,y_2,z_2) are set up in the two bodies with the center of the line of contact as a common origin. Coordinate axes (x_1,y_1) and (x_2,y_2) of the two systems are identical and lie in the tangent plane of initial contact. For convenience the x axis is directed along the initial line of contact (Fig. 1). In what follows, subscript 1 refers to the roller and subscript 2 refers to a contacting cylinder (e.g., a shaft).

The governing equation of three-dimensional elastic contact is given as

$$k \int_\Omega \frac{p(x',y')dx'dy'}{[(x-x')^2 + (y-y')^2]^{1/2}} - \delta + f_1(x,y) + f_2(x,y) = e' \quad (2)$$

where k is defined [9] as

$$k = \frac{1-\nu_1^2}{\pi E_1} + \frac{1-\nu_2^2}{\pi E_2} \quad (3)$$

ν and E denote Poisson's ratio and Young's modulus; $p(x',y')$ is the normal pressure over the contact region Ω, and δ is the relative approach of the centerlines of the two bodies. $z_1 = f_1(x,y)$ and $z_2 = f_2(x,y)$ define the surface profiles of the roller and the shaft. The relative separation e' should vanish inside the contact region Ω, and it should be a small positive quantity outside of it, i.e.,

$$e' = 0 \text{ for } (x,y) \text{ inside and on } \Omega \quad (4a)$$

$$e' > 0 \text{ for } (x,y) \text{ outside of } \Omega \quad (4b)$$

Equations (2)–(4) define the three-dimensional contact problem. A major obstacle in the solution of this problem is the lack of knowledge of the domain of integration, Ω. The region Ω must be such that the integral inequality (4b) is satisfied. As a first approximation to Ω, Singh [7] proposed that the interpenetration curve described by

$$f_1(x,y) + f_2(x,y) = d \quad (5)$$

be used as a tentative boundary for Ω. Equation (5) defines the projection, on the (x,y) plane, of the space curve formed by the hypothetical interpenetration of the two bodies due to a relative rigid-body translation through a distance d, referred to as the interpenetration distance.

For different values of d a family of interpenetration curves is generated. If an arbitrary member of this family is chosen as a tentative contact boundary for a region Ω^*, the resulting integral equations (2) and (4a) can be solved for the pressure $p(x',y')$ and the approach δ. The validity of the chosen region may then be determined by examining the inequality (4b). If inequality (4b) is satisfied, then Ω^* is an acceptable contact region. If not, then Ω^* should be modified and equations (2) and (4a) must be solved again. The details of this iterative solution, and a verification of its accuracy, can be found in Singh [7] and Singh and Paul [6]. The integral equation (2), subject to condition (4a), may be solved numerically in the manner described below.

The contact region is subdivided into small cells, and the pressure in each cell is assumed to be constant. The centroid of each cell is considered a field point. For field point i (coordinate x_i,y_i) equation (2) becomes

$$k\, p_i \int_{A_i} \frac{dx'\,dy'}{[(x'-x_i)^2 + (y'-y_i)^2]^{1/2}} + k \sum_{\substack{j=1 \\ j\neq i}}^{n} p_j \int_{A_j} \frac{dx'\,dy'}{[(x'-x_i)^2 + (y'-y_i)^2]^{1/2}} - \delta + f_1(x_i,y_i) + f_2(x_i,y_i) = e' \quad (6)$$

where A_i denotes the region of cell i. The first integral in equation (6) has a singularity in the integrand, but the integral may be obtained by elementary integration for polygonal cells. The second integral is given approximately as

Nomenclature

A_i = region of cell i
A = constant in Palmgren's formula
d = interpenetration
e' = relative separation, equation (4)
E_1, E_2 = Young's moduli of roller and shaft, psi
$f_1(x, y)$
$f_2(x, y)$ = profile function of the contacting elements
F = normal load, lb
k = elastic parameter, equation (3)
l = straight length of roller, in. (see Fig. 1)
P_i = pressure in cell i
$p(x, y)$ = pressure field
R_1, R_2 = radii of crowned roller and shaft, respectively, in.
R_c = crown radius, in.
δ = diametral compression, in.
δ_p = diametral compression in equation (1), in.
ν_1, ν_2 = Poisson's ratio of roller and shaft, respectively
ϵ = relative error
Ω = contact region

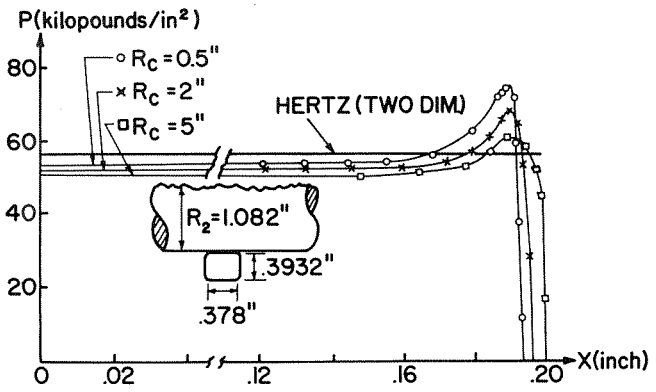

Fig. 3 Pressure distribution, crowned roller pressed against a shaft, F = 86.4 lb

$$I_{ij} = \int_{A_j} \frac{dx'\,dy'}{[(x' - x_i)^2 + (y' - y_i)^2]^{1/2}} \doteq \frac{A_j}{[(x_i - x_j)^2 + (y_i - y_j)^2]^{1/2}} \quad (7)$$

Equation (7) is shown in Singh [7] to be an excellent approximation when square cells are used. Thus equation (2) is transformed into a set of linear algebraic equations. These equations turn out to be extremely unstable, and a direct numerical solution gives meaningless results. A stabilization procedure called the method of functional regularization was developed to surmount this difficulty. A complete description of the theory may be found in Singh [7] or Singh and Paul [6, 10].

For an assumed interpenetration d, the contact region is defined, via equation (5), by

$$d = \frac{y^2}{2}\left(\frac{1}{R_1} + \frac{1}{R_2}\right) \qquad -\frac{l}{2} \le x \le \frac{l}{2} \quad (8)$$

$$d = \frac{(x - \frac{l}{2})^2}{2R_c} + \frac{y^2}{2}\left(\frac{1}{R_1} + \frac{1}{R_2}\right) \qquad x > l/2 \quad (9)$$

The semiwidth b of the straight portion of the contact region is given by an elementary calculation as

$$b = [2d/(R_1^{-1} + R_2^{-1})]^{1/2} \quad (10)$$

Having established a tentative contact region, the next step is to subdivide this region into n cells and to assume that the pressure in cell i is equal to a constant p_i.

Square cells are preferred over other configurations because of their symmetry. The error involved in discretization of the integral operator, equation (5), is more evenly distributed with a square cell network than with other shapes. This is discussed further in the Appendix.

For industrial roller bearings ($l/R_1 \approx 1.6$ or more), the aspect ratio A' of the contact region is as high as 400 for loads that induce peak pressures of the order of 40,000 psi. It is obvious that one quadrant of Ω can be covered by a network of approximately $\frac{1}{4}\,m^2A'$ square cells, where m is the number of cells along the short dimension. Thus an extremely large number of square cells appear to be needed to discretize the region. However, it is known from the physics of the problem that pressure is nearly independent of x except in the vicinity of the crowned surface. Therefore it might be thought that it is profitable to use elongated rectangular cells in that portion of the contact region that is far from the crowned surface, and to use a very fine square grid in the neighborhood of the crowned surface. However, the approximation for the integral $\int dA/r$, equation (7), introduces large error for integrals over rectangular cells when the field point is located near the longer side of the rectangle. (For example, in Fig. 2 the integral over cell 15 will be inaccurate if the field point is located in cell 1.) An estimate of the error involved in using the A/r approximation is given in the Appendix, where it is also shown that for those cases where the A/r approximation is inadmissible an analytical expression for the integral $\int dA/r$ is available.

In this way the discretized set of equations, corresponding to equation (6), is obtained, and the functional regularization method may be employed to solve this set of equations. A large number of problems were solved using a wide range of crowning radii and normal loads. A brief description of the conclusions is given below.

1 Even with the modified integration procedure for rectangular cells, cells with aspect ratios larger than 15 give rise to an inadequate set of equations that could not be regularized to give a physically meaningful solution.

2 For light loads the aspect ratio of the contact region is very large, and in such instances the discretized coefficient matrix may be of very high order. This may cause storage problems in small computers. In such cases the coefficient matrix is condensed by assuming the physically plausible result that the pressure is a very weak function of the x coordinate except in the vicinity of the crowned surface. Hence the pressure at field points with the same y coordinate will be equal except near the edge of the larger dimension of the contact region. For example, in Fig. 2 the pressure at field points 1, 2, 3, and 4 can safely be assumed to be equal. This has the effect of reducing the number of the unknowns in the problem and condensing the coefficient matrix to a manageable size. Numerical results for several problems show that the pressure variation along the y direction can be closely represented by

$$p(x, y) = P(x)\left[1 - \left(\frac{y}{f(x)}\right)^2\right]^{1/2} \quad (11)$$

where $f(x)$ defines the ordinate of the contact boundary.

3 The pressure rises steeply near the blending point. As would be expected, the peak value decreases with increasing values of R_c.

4 In the cases investigated to date it was found that the interpenetration curves constitute acceptable contact boundaries, and no iteration on the boundary was necessary.

Numerical Examples

Example 1: Roller pressed against a shaft: It will be assumed that a steel roller is pressed against a steel shaft.[2] Dimensions typical of a roller bearing (Harris, [1], p. 54) are

R_1 = roller radius = 0.1966 in.
R_2 = shaft radius = 1.082 in.
l = straight length of roller = 0.378 in.
$E_1 = E_2 = E = 30 \times 10^6$ psi
$\nu_1 = \nu_2 = \nu = 0.3$

The pressure distribution for contact between the roller and the shaft is shown in Fig. 3 for crown radii R_c = 0.5, 2, and 5 in. and load F = 86.4 lb. The Hertzian solution for infinite-length rollers predicts a peak pressure p_H given by

$$p_H = 0.418\left[\frac{FE(R_1 + R_2)}{lR_1R_2}\right]^{1/2} \quad (12)$$

In Fig. 3 the Hertzian pressure is based on the straight length l = 0.378 in. of the roller for a constant force F = 86.4 lb. For a crowned roller of equal straight length, the effective length of contact is larger, resulting in a pressure lower than p_H in the central region. The larger the crown radius the larger the effective length of contact, and hence the smaller the pressure in the central region for a given thrust F. On the other hand, the peak stress increases rapidly with decreasing crown radius, as is to be expected.

[2] The rollers of needle bearings often ride directly on the shaft. For roller bearings the shaft in question is a composite shaft that includes the inner race of the bearing.

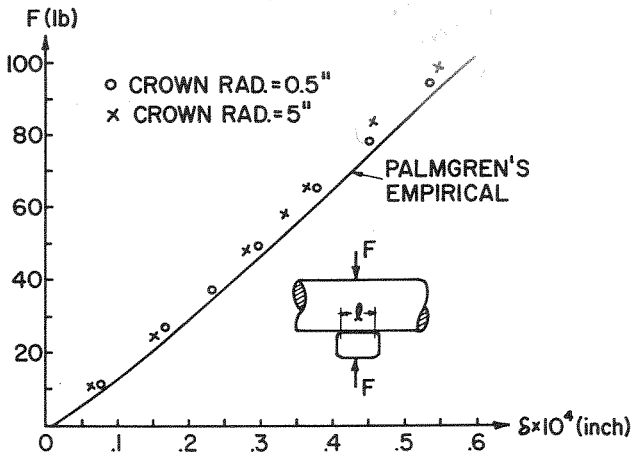

Fig. 4 Load vs. approach, crowned roller, straight length = 0.378 in.

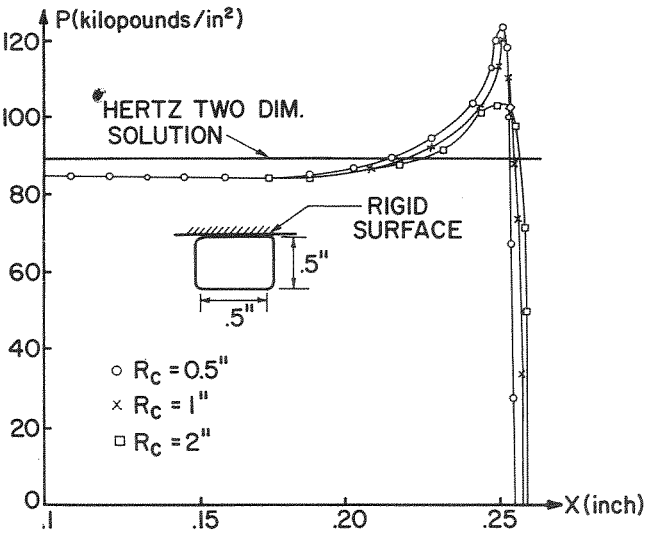

Fig. 5 Pressure distribution, crowned roller pressed against a rigid plane, F = 225 lb

The load-vs.-deflection relationships for R_c = 5 and 0.5 in. are shown in Fig. 4. Palmgren's empirical relation, equation (1), is also shown for comparison. Note that the crown radius has only a small effect on the approach because of the highly localized stress concentration associated with crowning. For the cases investigated, Palmgren's empirical formula predicts a reasonable, but consistently higher, approach than the more accurate numerical procedure (a typical difference is about 5 percent).

Example 2: A crowned roller pressing against a rigid plane:

$$\begin{aligned} R_1 &= \text{radius of roller} = 0.25 \text{ in.} \\ l &= \text{straight length} = 0.5 \text{ in.} \\ E_1 &= 30 \times 10^6 \text{ psi} \\ \nu &= 0.3 \\ F &= 225 \text{ lb} \end{aligned}$$

The pressure distribution along the x axis (y = 0) is shown in Fig. 5 for R_c = 0.5, 1, and 2 in.

Conclusions

A method has been developed for calculating the stresses produced by crowned rollers. The stresses are seen to be appreciably greater than those produced by the Hertz analysis for infinite-length bearings. To the best of our knowledge this is the first published solution that is based upon the equations of elasticity and includes the effect of the crown radius and the finite roller length. In addition to the complete pressure field, the relative approach and the contact region have been found.

We have also verified, over a limited range of parameters, Palmgren's empirical formula for the approach. Palmgren's predicted approach (which does not account for crowning) was found to be within 5 percent of the numerically calculated values in most cases. The computation procedure is extremely fast and inexpensive. The method presented in this work may be used as a guide to the specification of crowning radii and to the prediction of bearing life.

References

1 Harris, T. A., *Rolling Bearing Analysis*, Wiley, N. Y., 1966.

2 Harris, T. A., "Effect of Misalignment on the Fatigue Life of Cylindrical Roller Bearings Having Crowned Rolling Members," *Journal of Lubrication Technology*, TRANS. ASME, Series F, Vol. 91, No. 2, Apr. 1969, pp. 294–300.

3 Cheng, H. S., "List of Theses Topics in Tribology," *Journal of Lubrication Technology*, TRANS. ASME, Series F, Vol. 94, No. 2, Apr. 1972, pp. 107–111.

4 Palmgren, Arvid, *Ball and Roller Bearings*, Burbank and Co., Philadelphia, Pa., 1959.

5 Moyar, G. J., and Morrow, JoDean, "Surface Failure of Bearings and Other Rolling Elements," University of Illinois Engineering Experiment Station Bulletin No. 468, 1964.

6 Singh, K. P., and Paul, B., "Numerical Solution of Non-Hertzian Elastic Contact Problems," (to be published in *Journal of Applied Mechanics*).

7 Singh, K. P., "Contact Stresses in Elastic Bodies with Arbitrary Profiles," PhD thesis, University of Pennsylvania, Philadelphia, Pa., 1972.

8 Kalker, J. J., "A Minimum Principle for Frictionless Elastic Contact With Application to Non-Hertzian Half-Space Contact Problems," *Journal of Engineering Mathematics*, Vol. 6, 1972, pp. 193–206.

9 Timoshenko, S. P., and Goodier, J. N., *Theory of Elasticity* (2nd ed.), McGraw-Hill, New York, N. Y., 1951.

10 Singh, K. P., and Paul, B., "A Method for Solving Ill-Posed Integral Equations of the First Kind," *Computer Methods in Applied Mechanics and Engineering*, Vol. 2, 1973, pp 339–348.

APPENDIX

General Rectangular Cells

An important advantage of using square cells is that the A/r approximation, equation (7), may be used without introducing errors so great as to prohibit the use of the regularization method. When rectangular cells are used the A/r approximation may become unreliable. A quantitative measure of the error in equation (7) will be derived here.

Let us consider the integral $\int dA/r$, with r measured from a field point P over a rectangle of sides $2a$ and $2b$, where the point P is the centroid of an adjacent identical cell (Fig. 6*a*). We seek

$$\omega = \int_{EFCD} \frac{dA}{r} = \int_{ABCD} \frac{dA}{r} - \int_{ABFE} \frac{dA}{r} \tag{13}$$

Both integrals on the right-hand side of equation (13) can be computed from the general case depicted in Fig. 6*b*, with a suitable choice of $\bar{a}$ and $\bar{b}$. The required integral corresponding to Fig. 6*b* is given by elementary integration.

$$\int_{AB\bar{C}\bar{D}} \frac{dA}{r} = \bar{a} \ln \frac{(\bar{a}^2 + 4\bar{b}^2)^{1/2} + 2\bar{b}}{(\bar{a}^2 + 4\bar{b}^2)^{1/2} - 2\bar{b}} + 2\bar{b} \ln \frac{(\bar{a}^2 + 4\bar{b}^2)^{1/2} + \bar{a}}{(\bar{a}^2 + 4\bar{b}^2)^{1/2} - \bar{a}} \tag{14}$$

Introducing the notation

$$n = a/b \tag{15}$$

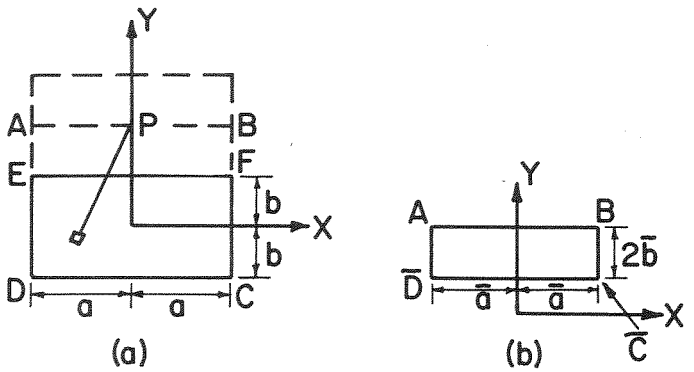

Fig. 6 Field point and adjacent rectangles

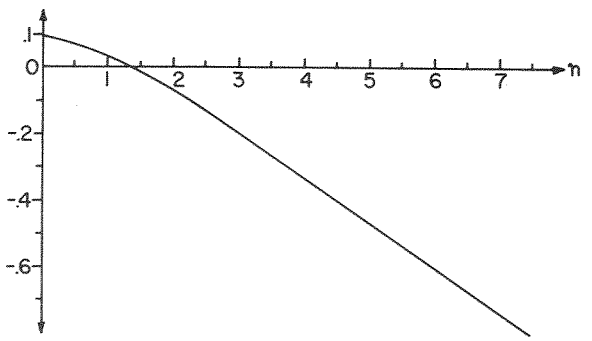

Fig. 7 Relative error vs. aspect ratio

in equation (14) and utilizing equation (13) we find

$$\omega = \int_{EFCD} \frac{dA}{r} = b\Big[n \ln \frac{(n^2+9)^{1/2}+3}{(n^2+9)^{1/2}-3} + 3 \ln \frac{(n^2+9)^{1/2}+n}{(n^2+9)^{1/2}-n} - n \ln \frac{(n^2+1)^{1/2}+1}{(n^2+1)^{1/2}-1} - \ln \frac{(n^2+1)^{1/2}+n}{(n^2+1)^{1/2}-n} \quad (16)$$

If the A/r approximation equation (7) is used, then

$$\omega^* = \int \frac{dA}{r} = \frac{A}{r_c} = \frac{4nb^2}{2b} = 2nb \quad (17)$$

The relative error is given by

$$\epsilon = \frac{\omega - \omega^*}{\omega} \quad (18)$$

Equations (16), (17), and (18) can be used to determine ω, ω^*, and ϵ as a function of the aspect ratio n. Figure 7 shows ϵ as a function of η. It is of some interest to note that the error may be as high as 100 percent for $n \approx 10$.

Figure 7 reveals the fact that a square-cell layout is relatively good from the standpoint of A/r approximation. A rectangular cell with $\eta \approx 1.35$ is ideal for approximating the integral over cells that lie adjacent to the longer side. For these cells, A/r approximation gives zero error. However, for the cells that lie adjacent to the shorter side the error is 5.81 percent. A uniform square mesh has a uniform error of 3.665 percent, for adjacent cells. Note that this error of 3.7 percent applies only to a small patch of the total contact region Ω and therefore contributes a much smaller net discretization error to the overall system matrix.

Printed in U. S. A.